

Spontaneous fluxon production in annular Josephson tunnel junctions in the presence of a magnetic field

R. Monaco*

*Istituto di Cibernetica del C.N.R., 80078 Pozzuoli, Italy
and Unita' INFM-Dipartimento di Fisica, Universita' di Salerno, 84081 Baronissi, Italy*

M. Aaroe[†] and J. Mygind

Department of Physics, B309, Technical University of Denmark, DK-2800 Lyngby, Denmark

R. J. Rivers[‡]

Blackett Laboratory, Imperial College London, London SW7 2AZ, United Kingdom

V. P. Koshelets[§]

Institute of Radio Engineering and Electronics, Russian Academy of Science, Mokhovaya 11, Building 7, 125009 Moscow, Russia

(Received 14 July 2007; revised manuscript received 15 December 2007; published 21 February 2008)

We report on the spontaneous production of fluxons in annular Josephson tunnel junctions during a thermal quench in the presence of a symmetry-breaking magnetic field. The dependence on field intensity B of the probability \bar{f}_1 to trap a single defect during the N - S phase transition depends drastically on the sample circumferences. We show that this can be understood in the framework of the same picture of spontaneous defect formation that leads to the experimentally well attested scaling behavior of \bar{f}_1 with quench rate in the absence of an external field.

DOI: 10.1103/PhysRevB.77.054509

PACS number(s): 74.50.+r, 03.65.Yz, 03.70.+k, 05.70.Fh

I. SPONTANEOUS FLUXON PRODUCTION IN AN EXTERNAL FIELD

Some time ago, it was proposed by Kibble¹ and Zurek^{2,3} that the domain structure after a continuous phase transition is determined by its causal horizons. Since then, there has been a sequence of experiments in condensed matter systems to attempt to confirm this by counting the topological defects produced at a quench, whose number can be correlated to phase boundaries. Such confirmation lies in the predicted scaling behavior of the average defect separation $\bar{\xi}$ at the time of their production as a function of the quench time (inverse quench rate at the critical temperature T_c) τ_Q . Supposing that the “equilibrium” correlation length $\xi_{eq}(T)$ of the order-parameter field and its relaxation time $\tau(T)$ diverge at $T=T_c$ as

$$\xi_{eq}(T) = \xi_0 \left| 1 - \frac{T}{T_c} \right|^{-\nu}, \quad \tau(T) = \tau_0 \left| 1 - \frac{T}{T_c} \right|^{-\gamma},$$

simple causal arguments predict behavior of the form¹⁻³

$$\bar{\xi} \propto \xi_0 (\tau_Q / \tau_0)^\sigma, \quad (1)$$

where the scaling exponent $\sigma > 0$ belongs to universality classes determined by the (adiabatic) critical exponents ν and γ , and ν , γ , ξ_0 , and τ_0 depend on the detailed microscopic behavior of the system. The coefficient of proportionality in Eq. (1) is an efficiency factor which varies with the system, from a few percent for high temperature superconductors^{4,5} to full efficiency for superfluid ³He.^{6,7}

In the past several years, we have performed a set of experiments⁸⁻¹¹ on planar annular Josephson tunnel junctions (JTJs) to test the scaling law (1). Specifically, a planar Jo-

sephson junction comprises two superconducting films separated by an insulating oxide layer. We assume continuity in the density of Cooper pairs across the oxide, but allow for a discontinuity ϕ in the phase of the effective order-parameter field. Once the transition is completed, the lossless Josephson current density is $J=J_c \sin \phi$, for critical current density J_c . For JTJs, the defects are fluxons (or antfluxons) corresponding to a change $\Delta\phi = \pm 2n\pi$ in ϕ along the oxide layer.¹² The integer $\pm n$ is the so-called winding number. The Swihart velocity provides the requisite causal horizons.¹³

Most simply, for small annuli of circumference $C \ll \bar{\xi}$, the trapping probability f_1 for finding a fluxon (or f_{-1} of finding an antfluxon) is taken to be

$$f_1 = f_{-1} = C/\bar{\xi} \propto (C/\xi_0)(\tau_Q/\tau_0)^{-\sigma}. \quad (2)$$

In our experiments, we measure $\bar{f}_1 = f_1 + f_{-1}$, the likelihood of seeing one fluxon or antfluxon. We have carried out statistical measurements to determine the dependence of \bar{f}_1 on τ_Q for a large number of high quality annular Josephson tunnel junctions (AJTJs) with circumferences varying from 0.5 mm to 3.14 mm. All samples had equal critical current density $J_c(T=0) \approx 60$ A/cm² [corresponding to a Josephson penetration depth $\lambda_J(T=0) \approx 50$ μ m], yielding the same ξ_0 and τ_0 . The quenching time τ_Q could be changed over several orders of magnitudes from tens of milliseconds to tens of seconds, using the methods described in Refs. 10 and 11.

In Fig. 1, we show $\bar{f}_1(\tau_Q)$ for annuli of radii, 0.5 mm (lower plot) and 1.5 mm (upper plot). The results for the larger annulus have not been shown before. There is no doubt that, for small $C/\bar{\xi}$, the probability \bar{f}_1 of finding a single fluxon shows scaling behavior of the type (2), with

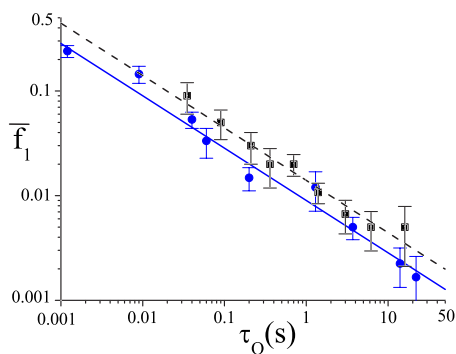


FIG. 1. (Color online) Log-log plot of the frequency \bar{f}_1 of trapping single fluxons versus the quenching time τ_Q for an AJTJ of circumference 0.5 mm (closed circles) and for an AJTJ with circumference 1.5 mm (closed squares). The best fits through the data (solid and dashed lines) show that scaling with $\sigma=0.5$ is totally robust. Both samples had equal critical current density J_c .

$\sigma=0.5$ to high accuracy; some of whose details were given in Refs. 10 and 11. This value of σ is as we would expect for realistic junctions for which the fabrication leads to a proximity effect^{14,15} and for which the Swihart velocity does not show complete slowing down. The efficiency factor is approximately unity for the smaller annulus. More details are given in Ref. 11.

What concerns us in this paper is how fluxons form in the presence of an externally applied magnetic field B that explicitly breaks the symmetry of the theory, whereby $f_1 \neq f_{-1}$. This is a crucial ingredient in the analysis of *unbiased* fluxon production in JTTs because, despite our best efforts, we cannot preclude the possibility of stray magnetic fields in the experimental equipment (e.g., a magnetized screw or an incomplete shielding of earth's magnetic field). In fact, in presenting the data in Fig. 1, we have taken the effects of static stray fields empirically into account, by applying an external field until such stray fields are neutralized. It is only then that we obtain Eq. (2). In all cases, the external magnetic field B was applied perpendicular to the junction plane. This choice of field orientation is mainly due to the fact that a transverse field (due to demagnetization effects) is more effective, by almost two orders of magnitude, than an in-plane field in modulating the junction critical current I_c (Ref. 16) and trapping frequency. Furthermore, under particular conditions,¹⁷ a transverse magnetic field allows to discriminate between fluxons and antifluxons.

As a result, we have built up a substantial collection of data showing the dependence of \bar{f}_1 on *both* τ and B , which we shall discuss in the remaining sections. In particular, we shall concentrate on two representative data sets that refer to high quality Nb/Al_{ox}/Nb-Nb AJTJs quenched at the same quench rate ($\tau_Q=5$ s), but having different circumferences, i.e., $C=0.5$ mm and $C=2.0$ mm, shown in Figs. 2 and 3, respectively. Details of the samples' electrical and geometrical parameters and of the experimental setup can be found in Ref. 11.

We observe that the increase in circumference has a dramatic effect on the single trapping frequency \bar{f}_1 . For the 0.5 mm long AJTJ, we find a central minimum with two side

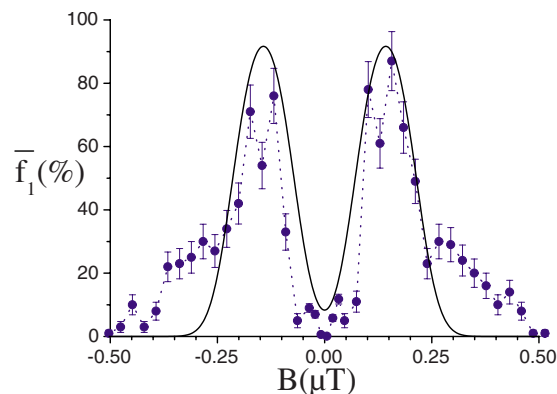


FIG. 2. (Color online) Dependence of the single fluxon trapping frequency \bar{f}_1 for quench time $\tau_Q=5$ s for an AJTJ of circumference $C=0.5$ mm in the presence of a magnetic field B perpendicular to the barrier plane. The solid line corresponds to the case $N=1$ in $\bar{f}_1(N, \bar{n})$ of Fig. 5, as derived from Eq. (22).

peaks. Such a double-peaked data set has been used for any single data point in Fig. 1, with \bar{f}_1 being read off from the central minimum, typically displaced slightly from $B=0$ because of the aforementioned stray fields in the equipment (typically several tens of nT).

On the other hand, for the 2.0 mm long sample (not represented in Fig. 1), we only have a central peak. Superficially, this is strange, since it shows that the probability of seeing a single fluxon *decreases* as the external field increases, but we shall understand this as a consequence of an increased ability to create more than one fluxon. We note that the values of the magnetic field required to change \bar{f}_1 significantly are very small when compared to the field values needed to modulate the Josephson current I_c of the samples, whose first minimum occurs at field values of several μT . Further, the larger the ring size the larger is the effect of a given magnetic field.

In the remainder of this paper, we shall show how the results of Figs. 2 and 3 can be understood, and qualitatively

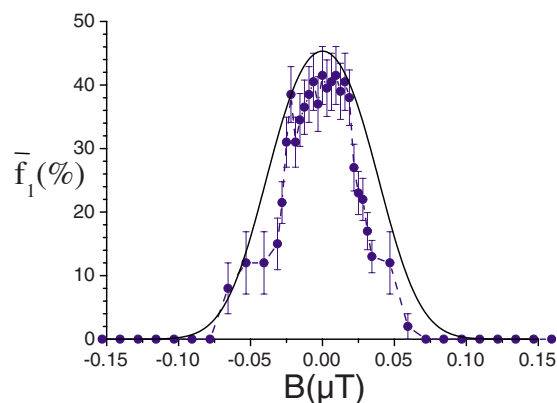


FIG. 3. (Color online) Dependence of \bar{f}_1 for quench time $\tau_Q=5$ s for an AJTJ of circumference $C=2.0$ mm in the presence of a magnetic field B perpendicular to the barrier plane. The solid line corresponds to the case $N=16$ in $\bar{f}_1(N, \bar{n})$ of Fig. 5, as derived from Eq. (22).

predicted, in a framework that implies the scaling behavior of Fig. 1. As such, these results are mutually supportive but require an alternative formulation of the Kibble-Zurek (KZ) scenario, which we now provide.

II. CAUSALITY VERSUS INSTABILITY

At first sight, the results for fluxon production in an external field have little or nothing to do with the Kibble-Zurek scenario. However, the original scenario of bounding domains by causal horizons is just one way of saying that, qualitatively, systems change as fast as is possible. From a different viewpoint, we know that continuous transitions (like the one here) proceed by the exponential growth of the amplitudes of unstable long-wavelength modes of the system. This growth is strongly suppressed by self-interaction once the system is close to the ground states of its symmetry-broken phase.

Exponential growth is as fast as it gets, corresponding to linearizing the equations of motion. Thus, provided there is enough time for such rapid growth before back reaction (self-interaction) stops it, we can understand how systems can change as fast as is possible without invoking causal horizons directly. There is a corollary to this. The linear behavior of the order-parameter fields, while the transition is taking place, follows from their behaving as Gaussian random variables. In fact, for an idealized situation in which amplitude growth is stopped by implementing a rapid back reaction that chokes off growth instantaneously, it can be shown^{18–20} that the assumption of Gaussianity leads to scaling behaviour like that of Eq. (1), with the same values of σ as would be obtained from causal bounds. What may seem surprising is that, even when back reaction is included more realistically, numerical simulations^{21–23} show that the behavior is still essentially the same. The σ exponents of causal reasoning are recovered. There are, however, two major differences between fastest amplitude growth and causal bounds. The growth starts after the transition has begun, whereas causal bounds can be imposed both *before* or *after* the transition has begun, usually to the same effect.^{2,3} Numerical simulations show,^{22,23} without a doubt, that it is the behavior of the system after the transition has begun that determines the domain structure. This is necessary in our context since, with no Josephson effect for $T > T_c$, we could not have invoked causality before the transition. Further, the assumption of Gaussianity gives us more than causality, in that it reintroduces the role of the Ginsburg temperature, at which thermal fluctuations become important, where appropriate. This provides one natural explanation for the failure to observe vortices in quenches of ⁴He,¹⁹ while, by a similar argument, permitting spontaneous vortex production in ³He (Refs. 6 and 7) and superconductors.⁵

However, since equations of motion are, by construction, causal, these viewpoints are largely complementary once these caveats are taken into account. When appropriate, we will invoke both mechanisms in our subsequent discussion.

The simulations cited above are largely for systems with global symmetry breaking, simpler than superconductors. In fact, although local breaking gives a very different domain

structure, the idea of the transition being driven by instabilities survives. Again, the exponents are those of causal arguments²⁴ except that there is an *additional* mechanism²⁵ for the spontaneous production of flux in which magnetic field just freezes in by itself, with behavior very different to that of Eq. (1). For annular JTJs, this further mechanism does not arise because of the thinness of the oxide layer through which fluxons protrude and the scaling behavior of Eqs. (1) and (2) is a clean prediction.

III. BEYOND THE LINEAR REGIME ($B=0$)

Suppose that there is no external symmetry-breaking field. As long as f_1 is significantly smaller than unity, we expect the *linear* log plot in τ_Q , as seen in Fig. 1. However, with f_1 bounded by unity, the linear behavior will soon break down for increasingly fast quenches. Once $\bar{\xi} = O(C)$, the trapping probability f_m of finding net fluxon number m (fluxons minus antifluxons) increases for $m > 1$, forcing f_1 to decrease. For the remainder of this section, we shall extend Eq. (2) to predictions for f_1 and higher f_m across the whole range of $C/\bar{\xi}$.

Since the KZ scenario is appropriate for $B=0$, this is an ideal testing ground for our two approaches. We shall elaborate on these in turn and see that, for many purposes, they give almost indistinguishable results.

A. Independent domains and Gaussian probabilities

In the spirit of the KZ scenario, a simple but informative first guess as to how f_1 and other f_m behave across the whole range of $C/\bar{\xi}$ is to divide the annulus into $N \geq 2$ independent (causal) domains in each of which the Josephson phase ϕ is a constant. We assume that there is no correlation between the values of ϕ in adjacent domains but, in calculating the total phase change $\Delta\phi$ around the annulus, the geodesic rule is adopted.²⁶ This means that, when jumping from one domain to the other, the shortest path in phase will be taken. The result of a quench is then modeled as having the system divided up into N domains, each with a randomly chosen phase. There is nothing in this ansatz peculiar to JTJs, and it is equally applicable to superconductors. As such, it is an idealization of a superconducting loop, made out of Josephson junctions in series, that has been the object of spontaneous flux generation.⁴

Let $G_M(\Delta\phi)$ be the probability that the change in phase ϕ is $\Delta\phi$ after M domain boundaries. If the system is made of only two domains, then the lack of phase correlation requires

$$G_1(\Delta\phi) = \frac{1}{2\pi} \quad \text{for } -\pi < \Delta\phi < \pi,$$

$$= 0 \quad \text{for } |\Delta\phi| > \pi.$$

In fact, the approach of using the KZ picture to set up discrete domains in which the order-parameter field can take random values is one that has been used repeatedly for counting defects, at least since its introduction by Vachaspati and Vilenkin²⁷ for counting cosmic strings (vortices) in the

early universe. This adopts an earlier use of causal horizons by Kibble,²⁸ from which Ref. 1 evolved.

On increasing N , $G_N(\Delta\phi)$ is determined by $N-1$ self-convolutions of G_1 :

$$G_N = \underbrace{G_1 * \dots * G_1}_{N-1 \text{ times}}$$

Applying the geodesic rule for the final step in phase (from domain N back to domain 1), the probability of ending with a phase shift of $2\pi m$ (i.e., net fluxon number m) is

$$f_m(N) = \int_{-\pi+2m\pi}^{\pi+2m\pi} d\Phi G_N(\Phi) = 2\pi G_{N+1}(2m\pi), \quad (3)$$

where the last equality comes from the definition of G_N .

To bring this further into correspondence with the KZ scenario, we should identify the domain size as comparable to $C/\bar{\xi}$, i.e., $C = aN\bar{\xi}$, where $a = O(1)$. The value of a is not unity, since a discrete domain structure is only a crude approximation to a continuous phase at a continuous transition. Further, the result (1) assumes that the causal bound is saturated, and we have already commented on systems (e.g., high- T_c superconductors) for which the inefficiency of producing flux shows that this is not the case.⁵ To take general values of C and $\bar{\xi}$ into account, we need to generalize Eq. (3) to noninteger N .

$G_N(\Delta\phi)$ already shows rapid convergence to the Gaussian distribution that arises from the central limit theorem for $N \geq 2$. For such N , the obvious way to proceed is to adopt this central limit Gaussian distribution. That is, we assume that the total phase change $\Delta\phi$ around the annulus can be expressed as the sum of a random term Φ and a geodesic-rule correction $\delta\Phi$. If Φ has a normal distribution with average $\bar{\Phi} = 0$ and variance $\sigma^2(N)$, i.e.,

$$G_N(\Phi) = \frac{1}{\sqrt{2\pi\sigma^2(N)}} \exp\left(-\frac{\Phi^2}{2\sigma^2(N)}\right), \quad (4)$$

then a simple calculation enables us to identify Eq. (4) with the central limit distribution of the self-convolutions of G_1 , as described above, provided that

$$\sigma^2(N) = N\pi^2/3.$$

The probability to trap a net number m of defects will now be

$$f_m(N) = \int_{-\pi+2m\pi}^{\pi+2m\pi} d\Phi G_N(\Phi). \quad (5)$$

Experimentally, in the absence of any external field, the most important probabilities are for finding one fluxon or one antifluxon. The frequency of no trapping $f_0(N)$ is

$$f_0(N) = \int_{-\pi}^{\pi} G_N(\Phi) d\Phi = \operatorname{erf}\left(\frac{\pi}{\sqrt{2\sigma^2(N)}}\right), \quad (6)$$

and

$$f_{\pm 1}(N) = \int_{\pi}^{3\pi} \frac{d\Phi}{\sqrt{2\pi\sigma^2(N)}} \exp\left(-\frac{\Phi^2}{2\sigma^2(N)}\right). \quad (7)$$

Furthermore, for large $\sigma^2 \gg \frac{\pi^2}{2}$, say, $\sigma^2 \geq 20$, the trapping frequencies asymptotically approach zero as

$$f_{\pm m}(N) \approx \sqrt{\frac{2\pi}{\sigma^2(N)}} \exp\left(-\frac{2\pi^2 m^2}{\sigma^2(N)}\right). \quad (8)$$

Finally, in the same limit, the variance of the discrete variable n is

$$\sigma_n^2(N) = \sum_{n=-\infty}^{\infty} n^2 f_n(N) = \langle n^2 \rangle = \sigma^2(N)/4\pi^2. \quad (9)$$

For $N \leq 2$, we require a different approach and turn to the consequences of assuming Gaussian stochastic behavior.

B. Gaussian correlations

If x measures distance along the annulus, $\phi(x)$ is periodic (mod 2π). The fluxon number density (or winding number density) is

$$n(x) = \frac{1}{2\pi} \partial_x \phi(x), \quad (10)$$

whereby the net fluxon number n is

$$n = \int_0^C dx n(x) = \frac{1}{2\pi} \Delta\phi, \quad (11)$$

where $\Delta\phi$ is the change in ϕ .

For winding number density $n(x)$, the ensemble average of the net number of fluxons along an annulus of perimeter C , in the absence of an external field, is $\bar{n} = \langle n \rangle = 0$.

We do not need to adopt any particular form for $n(x)$. In the light of our earlier discussion, we now assume that it is a *Gaussian* variable until the transition is complete, whereby all correlation functions are determined by the two-point correlation function $\langle n(x)n(y) \rangle$. That is, all we shall need for probabilities is

$$\langle n^2 \rangle = \int_0^C dx dy \langle n(x)n(y) \rangle.$$

It follows that

$$\langle n^{2p} \rangle = \frac{(2p-1)!}{2^{p-1}(p-1)!} \langle n^2 \rangle^p. \quad (12)$$

If f_m is the probability of finding net winding number m taking both positive and negative values, then

$$\langle n^{2p} \rangle = \sum_{m=-\infty}^{\infty} m^{2p} f_m. \quad (13)$$

In order to invert Eq. (13), we construct the generating function $Z(z)$

$$Z(z) = \sum_{p=0}^{\infty} \frac{(-z^2)^p}{(2p)!} \langle n^{2p} \rangle = \exp(-z^2 \langle n^2 \rangle / 2),$$

from Eq. (12). On the other hand, from Eq. (13),

$$Z(z) = \sum_{p=0}^{\infty} \frac{(-z^2)^p}{(2p)!} \sum_{m=-\infty}^{\infty} m^{2p} f_m = \sum_{m=-\infty}^{\infty} f_m \cos mz.$$

That is, the f_m are the Fourier coefficients of the Gaussian. In particular,

$$f_0 = \frac{1}{2\pi} \int_{-\pi}^{\pi} dz \exp(-z^2 \langle n^2 \rangle / 2) \quad (14)$$

and

$$f_{\pm 1} = \frac{1}{2\pi} \int_{-\pi}^{\pi} dz \exp(-z^2 \langle n^2 \rangle / 2) \cos z,$$

respectively.

We observe that, for large $\langle n^2 \rangle$, where we can take the integration limits to infinity, the trapping probability falls off as

$$f_{\pm m} \approx \frac{1}{\sqrt{2\pi \langle n^2 \rangle}} \exp(-m^2 / 2 \langle n^2 \rangle).$$

In practice, this assumption of a Gaussian stochastic density can only be approximate, on two accounts. Less significantly, from our earlier comments, it ignores the nonlinearities of the system. More importantly, it does not fully accommodate the periodicity of the annulus, to which we shall return later. Nonetheless, it will be apparent as to which results are reliable.

In contrasting Gaussian correlations and Gaussian probabilities, we see that the definitions are dual to each other. In the limit of unrestricted integration (large N), they are identical if we identify

$$\langle n^2 \rangle = \sigma^2(N) / 4\pi^2 = N/12. \quad (15)$$

However, for small N , there will be differences, as we shall see.

On inserting Eq. (15), we find that the likelihood \bar{f}_1 of seeing one fluxon or antifluxon is

$$\bar{f}_1(N) = \frac{1}{\pi} \int_{-\pi}^{\pi} dz \exp(-z^2 N / 24) \cos z, \quad (16)$$

whereas, assuming Gaussian probability, from Eq. (5), we find

$$\bar{f}_1(N) = \operatorname{erf}\left(\frac{3\sqrt{3}}{\sqrt{2N}}\right) - \operatorname{erf}\left(\frac{\sqrt{3}}{\sqrt{2N}}\right). \quad (17)$$

We know that Eqs. (16) and (17) agree for large N but, as can be seen from Fig. 4, the qualitative and quantitative agreement is striking over the whole range.

In Fig. 4, we compare \bar{f}_1 as a function of N , as given by Eqs. (16) and (17) (dashed and dotted lines), respectively; the dots are the values of \bar{f}_1 according to the independent sector model for some integer values of N from Eq. (3). Agreement is already good at $N=2$ and very good at $N=4$.

However, the plots of Fig. 4 are somewhat deceptive for small N . This should not worry us since, although the analytic expression (17)

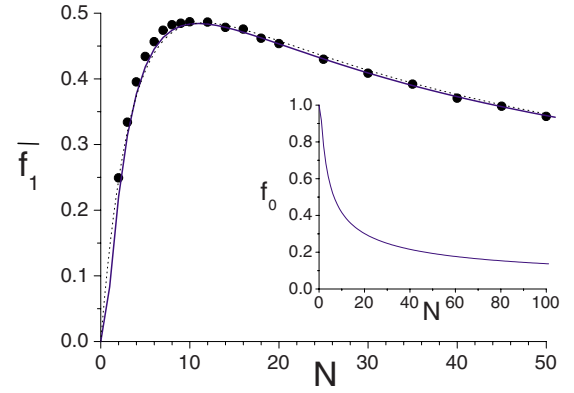


FIG. 4. (Color online) We display the probabilities $\bar{f}_1 = f_1 + f_{-1}$ as a function of N , as given by Eqs. (16) and (17) (dashed and dotted lines), respectively; the dots are the values of \bar{f}_1 according to the independent sector model for some integer values of N from Eq. (3). The maximum of \bar{f}_1 occurs at $N = N_c \approx 10.5$, for which value $\bar{f}_1 \approx 49\%$. The inset shows the probability \bar{f}_0 as a function of N , as given by Eq. (6), essentially indistinguishable from that by Eq. (19) at this scale.

$$\bar{f}_1(N) = O(\sqrt{N}) \exp(-3/2N), \quad (18)$$

vanishes faster than any power, Eq. (17) breaks down there by definition. On the contrary, $\bar{f}_1(N)$ of Eq. (16) is *linear* in N for small N , as we supposed in Eq. (2).

Finally, in the inset of Fig. 4, we also display $f_0(N)$, the probability of seeing no flux, for the case of Gaussian probabilities given in Eq. (6). Although we do not show it, at the scale of the plot, it is essentially indistinguishable from the result of assuming Gaussian correlations as given in Eq. (14),

$$f_0(N) = \sqrt{\frac{6}{\pi N}} \operatorname{erf}\left(\frac{\pi}{2} \sqrt{\frac{N}{6}}\right). \quad (19)$$

We can comfortably use either.

C. Consequences

In summary, the assumptions of Gaussian probabilities (as follows from the KZ picture) and Gaussian correlations are complementary, with the latter providing a (linear) interpolation of the other for $N \lesssim 2$ where the former breaks down.

The first observation is that, in both cases, the maximum probability $\bar{f}_1 = \bar{f}_c$ of seeing one fluxon *or* antifluxon is fractionally less than 50% (48.6%), occurring at $N = N_c \approx 10.5$. The assumption made in our JTJ papers is that \bar{f}_1 (which we have called f_1 in our papers) scales linearly with $N \propto C/\xi$, which we see is valid at best only until $\bar{f}_1 \approx 0.3$. We have already just about achieved this in the existing experiments but have not yet been able to quench fast enough to provide a direct test of the model predictions of Fig. 4. There is, however, a problem that stops us embracing the Gaussian correlation approach wholeheartedly, as we have presented it here. As we have noted, the assumption of Gaussian winding number density can only be approximated, since it does not

take periodicity (mod 2π) into account. We have seen that this does not matter in the calculation of f_0 and \bar{f}_1 .

However, for small annuli, there is a problem with Eq. (16) in that Fourier components $f_{\pm 2}(N)$ are slightly *negative* ($|f_{\pm 2}| < 0.01$) for very *small* N (with a similar problem for the very much smaller \bar{f}_4). On the other hand, by construction, the $\bar{f}_m(N)$ of Eq. (17) are automatically positive as they must be.

In a qualitative sense, it is of little consequence since, throughout the linear regime, the probability $\bar{f}_> = 1 - f_0 - \bar{f}_1$ of seeing more than one fluxon is very small but, as a matter of principle, we should impose periodicity to render the probabilities positive. We do not have a reliable model in which we can do this but we can get some idea by supposing that the phase ϕ moved in a double-well potential rather than the periodic $\cos \phi$ potential of the sine-Gordon fluxon. In that case, assuming Gaussian correlations, the density of defects is proportional²⁹ to $(f''(0)/f(0))^{1/2}$, where $f(x) = \langle \phi(x)\phi(0) \rangle$. It is now straightforward to impose periodicity, whereupon we find behavior similar to that of Eq. (18) for very small N , in that it vanishes faster than any power.³⁰ If that were to be equally applicable here, it is difficult to determine when such behavior might occur, since there is no sign of such a collapse in Fig. 1, but if this analogy is correct, it will repair the minor problem of small negative probabilities while leaving the similarity between the two approaches at a quantitative level. In particular, as long as we are not looking at the small- N behavior in too much detail, as we shall not hereafter, it becomes sensible to use the simpler Gaussian probabilities over the whole range.

IV. FLUXON PRODUCTION IN AN EXTERNAL FIELD B $\neq 0$

Let us now apply a perpendicular uniform magnetic field B to the AJTJ. This breaks the $\phi \rightarrow -\phi$ symmetry that is equally the reflection symmetry of the system in the plane of the barrier. Once superconducting, the AJTJ expels the magnetic field, but we assume that a small fraction ϵ of the applied field “leaks” in the radial direction through the barrier, forming fluxons. The effect of this field is to produce a non-zero average winding number $\langle n \rangle = \bar{n}(B)$.

The result is a shift in phase gradient along the annulus (coordinate x) of the form

$$\partial_x \phi \rightarrow \partial_x \phi + \frac{2e}{\hbar c} A_x,$$

where $A_x = A_x^+ - A_x^-$ is the jump in the vector potential across the oxide layer.

If $C = 2\pi R$ is the circumference of the ring, radius R , then the change in ϕ due to B is

$$\Delta \phi = \epsilon \frac{2e}{\hbar c} \oint \mathbf{dl} \cdot \mathbf{A} = \frac{\epsilon}{2\pi \hbar c} e C^2 B. \quad (20)$$

The change in fluxon number is

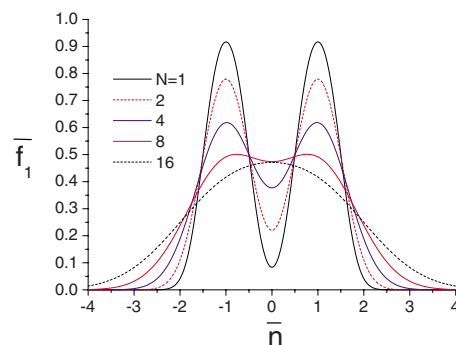


FIG. 5. (Color online) The values of $\bar{f}_1(N, \bar{n})$ as a function of \bar{n} for fixed N for several values of N ; $N=1, 2, 4, 8$, and 16 , according to Eq. (22).

$$\bar{n}(B) = \frac{1}{2\pi} \Delta \phi = \frac{\epsilon}{4\pi^2 \hbar c} e C^2 B. \quad (21)$$

[For future purposes, let us call B_1 the field value for which $\Delta \phi = 2\pi$, that is, $\bar{n}(B_1) = 1$.] When \bar{n} is small, ϵ adjusts in any individual experiment so as to make \bar{n} integer. As a first approximation, we take the fraction ϵ to be independent of B .

In the presence of external fields, we are not primarily interested in the small- N linear regime and it is sufficient to work with Gaussian probabilities. The natural extension of $G(\Phi)$ of Eq. (4) for an AJTJ in a perpendicular magnetic field B is that the phase distribution will still be normal with variance $\sigma^2[N, \bar{n}(B)] \propto N$, where we retain the definition of $N \propto C/\bar{\xi}$ of the previous section, but with nonzero average $\bar{\Phi}(B) = 2\pi \bar{n}(B)$:

$$G_{N, \bar{n}}(\Phi) = \frac{1}{\sqrt{2\pi\sigma^2(N, \bar{n})}} \exp - \frac{[(\Phi - \bar{\Phi}(B))]^2}{2\sigma^2(N, \bar{n})}.$$

The trapping probabilities in the presence of an external magnetic field will then be

$$f_m(N, \bar{n}) = \int_{-\pi+2m\pi}^{\pi+2m\pi} d\Phi G_{N, \bar{n}}(\Phi). \quad (22)$$

To a first approximation, we assume that $\sigma^2(N, \bar{n})$ is independent of $\bar{n}(B)$, as would follow from assuming Gaussian correlations, i.e., for integer \bar{n} , $f_{\bar{n}-m}(N, \bar{n}) = f_{\bar{n}+m}(N, \bar{n}) = f_{\pm m}(N, 0)$. This allows us to repeat the identification $\sigma^2(N)/4\pi^2 = N/12$.

As before, we are primarily interested in the probability of seeing a single fluxon or antifluxon, but now for fixed τ_Q (or N), as a function of B (or \bar{n}). Now, as far as $\bar{n} \neq 0$, then the symmetry is broken and $f_{+1}(N, \bar{n}) \neq f_{-1}(N, \bar{n})$. More precisely, in Fig. 5, we show $\bar{f}_1(N, \bar{n})$ as a function of \bar{n} for fixed N for several N , as derived from Gaussian distributions Eq. (22).

The main characteristics of Fig. 5 are the following:

(1) For $N < N_c \approx 10.5$, there is a double peak, corresponding to the ensemble average production of a single fluxon by the applied external magnetic field. This is understood as follows. Essentially, when, for $B = B_1$, we have $\bar{n} = 1$, the

zero-field no-trapping frequency $f_0(N,0)$ becomes the single fluxon trapping $f_{+1}(N,1)=f_0(N,0)$, giving the right hand peak for positive $\bar{n}\approx 1$; reversing the field, $f_{-1}(N,-1)=f_0(N,0)$ and we get the peak for negative $\bar{n}\approx -1$. The minimum value of \bar{f}_1 between the peaks is $\bar{f}_1(N)$, as given by the KZ scenario.

(2) As N increases to N_c , the height $\bar{f}_1(N,0)$ drops. The variance also increases, the Φ distribution gets broader and the two peaks in \bar{n} of $\bar{f}_1(N,\bar{n})$ merge at $N=N_c$ at the value $\bar{f}_c\approx 0.5$.

(3) As N increases beyond N_c , there is only a single peak centered on $\bar{n}=0$. We now see that the reason why the probability of seeing a fluxon *decreases* as $|B|$ increases is a consequence of an increased ability to create more than one fluxon.

The curves in Fig. 5 for $N=1$ and $N=16$ bear a strong resemblance to the experimental data shown in Figs. 2 and 3, respectively. They comply with the most simple qualitative test of our analysis, that the double peaks in Fig. 1 occur at a *higher* frequency than $\bar{f}_c\approx 50\%$, and the single peak in Fig. 2 at a *lower* frequency than 50%, as predicted. Further, we also found that the defect winding number flips when we move from the left to the right peak, as foreseen by both models. This discrimination between a trapped fluxon or antifluxon can be achieved by measuring the transverse magnetic field dependence of the junction critical current $I_c(B)$ (the details of this new effect and its theoretical interpretation will be reported elsewhere¹⁷).

More specifically, we note that the 2.0 mm long sample, being four times longer than the 0.5 mm long sample, according to Eq. (21), should be 16 times more sensitive to the externally applied magnetic field B , if $\epsilon(B)$ is independent of B and identical for both samples. There is, indeed, a strong difference in sensitivity, but only by a factor of 7–8, showing that these assumptions are approximate. What is more difficult to understand quantitatively is the 16-fold increase in N for a fourfold increase in perimeter. This requires the efficiency factor a relating N to C to vary by a factor of 4 between the samples or, more fundamentally, that N is not linear in C . Of itself, the latter does not change the scaling behavior of Eq. (2), but the scaling exponent σ . In Refs. 10 and 11, we showed that the observed value for σ was not that for idealized JTJs.¹³ We explained this as a consequence of

fabrication methods, but this reopens the issue.

To go further, and match the data profiles better, we need specific properties of JTJs, beyond the generics of the KZ picture (or Gaussian correlations). In particular, the assumption of $\sigma^2[N,\bar{n}(B)]$ being independent of $\bar{n}(B)$ is oversimple. More realistically,³¹ $\sigma^2[N,\bar{n}(B)]=\sigma^2(N,0)(1+k^2B^2)$, where $k^2\propto(\lambda_J/C)^2$, i.e., it is inversely proportional to the ring area and to the Josephson current density J_c , since $\lambda_J^2\propto 1/J_c$. Both are consistent with the experimental data, such as the flattening of \bar{f}_1 for small B field values and the fact that the peak amplitudes $f_{\pm n}(\pm B_n)$ strongly decrease with n , as we shall see elsewhere.

V. CONCLUSIONS

We have developed two complimentary theoretical approaches to understand the experimentally observed spontaneous production of fluxons on quenching annular JTJs in the presence of an externally applied transverse symmetry-breaking magnetic field B . They either assume Gaussian probabilities (as motivated by KZ causal horizons) or Gaussian correlation functions (as motivated by models for transitions based on the rapid growth of instabilities). Both of these approaches, which are, approximately, identical, lead to the same scaling behavior of Eq. (1), from which Eq. (2) follows in the appropriate regime.

The theory is able to nicely reproduce the double peak behavior of the likelihood f_1 to produce a single defect (fluxon) shown in Fig. 2 for a sample having a circumference equal to 0.5 mm and the single peak in Fig. 3 for a sample of circumference 2.0 mm. When we began experiments on fluxon production in an external symmetry-breaking field, we anticipated the behavior shown in Fig. 2, and not that of Fig. 3, which was initially incomprehensible. We now understand it, as a consequence of the ease of producing more than one fluxon in larger annuli. Specifically, our models do provide a good first approximation at a better than qualitative level and the experimental success of the Gaussian picture in describing the production of fluxons is of a piece with the scaling behavior so robustly demonstrated in Fig. 1.

ACKNOWLEDGMENTS

We thank Arttu Rajantie for helpful discussions. R.M. acknowledges the support of ESF under the COSLAB project and of CNR under the Short-Term Mobility 2007 program.

*roberto@sa.infn.it

†aaroe@fysik.dtu.dk

‡r.rivers@imperial.ac.uk

§valery@hitech.cplire.ru

¹T. W. B. Kibble, Phys. Rep. **67**, 183 (1980).

²W. H. Zurek, Nature (London) **317**, 505 (1985); Acta Phys. Pol. B **24**, 1301 (1993).

³W. H. Zurek, Phys. Rep. **276**, 177 (1996).

⁴R. Carmi, E. Polturak, and G. Koren, Phys. Rev. Lett. **84**, 4966 (2000).

⁵A. Maniv, E. Polturak, and G. Koren, Phys. Rev. Lett. **91**, 197001 (2003).

⁶C. Bauerle, Y. M. Bunkov, S. N. Fisher, H. Godfrin, and G. R. Pickett, Nature (London) **382**, 332 (1996).

⁷V. M. H. Ruutu, V. B. Eltsov, A. J. Gill, T. W. B. Kibble, M. Krusius, Y. G. Makhlin, B. Placais, G. E. Volovik, and W. Xu, Nature (London) **382**, 334 (1996).

⁸R. Monaco, J. Mygind, and R. J. Rivers, Phys. Rev. Lett. **89**, 080603 (2002).

⁹R. Monaco, J. Mygind, and R. J. Rivers, Phys. Rev. B **67**, 104506

- (2003).
- ¹⁰R. Monaco, J. Mygind, M. Aaroe, R. J. Rivers, and V. P. Koshelets, *Phys. Rev. Lett.* **96**, 180604 (2006).
- ¹¹R. Monaco, M. Aaroe, J. Mygind, R. J. Rivers, and V. P. Koshelets, *Phys. Rev. B* **74**, 144513 (2006).
- ¹²A. Barone and G. Paternó *Physics and Applications of the Josephson Effect* (Wiley, New York, 1982).
- ¹³E. Kavoussanaki, R. Monaco, and R. J. Rivers, *Phys. Rev. Lett.* **85**, 3452 (2000). R. Monaco, R. J. Rivers, and E. Kavoussanaki, *J. Low Temp. Phys.* **124**, 85 (2001).
- ¹⁴J. M. Rowell and P. H. Schmidt, *Can. J. Phys.* **54**, 223 (1976).
- ¹⁵A. A. Golubov, E. P. Houwman, J. G. Gijsbertsen, V. M. Krasnov, J. Flokstra, H. Rogalla, and M. Yu. Kupriyanov, *Phys. Rev. B* **51**, 1073 (1995).
- ¹⁶R. Monaco, M. Aaroe, J. Mygind, V. P. Koshelets, arXiv:cond-mat/0706070 (unpublished); *J. Appl. Phys.* **102**, 093911 (2007).
- ¹⁷R. Monaco, J. Mygind, M. Aaroe, V. P. Koshelets, (unpublished).
- ¹⁸G. Karra and R. J. Rivers, *Phys. Lett. B* **414**, 28 (1997).
- ¹⁹G. Karra and R. J. Rivers, *Phys. Rev. Lett.* **81**, 3707 (1998).
- ²⁰M. Bowick and A. Momen, *Phys. Rev. D* **58**, 085014 (1998).
- ²¹P. Laguna and W. H. Zurek, *Phys. Rev. D* **58**, 085021 (1998); P. Laguna and W. H. Zurek, *Phys. Rev. Lett.* **78**, 2519 (1997).
- ²²E. Moro and G. Lythe, *Phys. Rev. E* **59**, R1303 (1999).
- ²³N. D. Antunes, P. Gandra, and R. J. Rivers, *Phys. Rev. D* **73**, 125003 (2006).
- ²⁴A. Yates and W. H. Zurek, *Phys. Rev. Lett.* **80**, 5477 (1998); D. Ibaceta and E. Calzetta, *Phys. Rev. E* **60**, 2999 (1999).
- ²⁵M. Hindmarsh and A. Rajantie, *Phys. Rev. Lett.* **85**, 4660 (2000); A. Rajantie, *J. Low Temp. Phys.* **124**, 5 (2001).
- ²⁶S. Rudaz and A. M. Srivastava, *Mod. Phys. Lett. A* **8**, 1443 (1993).
- ²⁷T. Vachaspati and A. Vilenkin, *Phys. Rev. D* **30**, 2036 (1984).
- ²⁸T. W. B. Kibble, *J. Phys. A* **9**, 1387 (1976).
- ²⁹B. I. Halperin, *Physics of Defects*, Proceedings of Les Houches, Session XXXV 1980 NATO ASI, edited by R. Balian, M. Kléman, and M. Poirier (North-Holland, Amsterdam, 1981), p. 816.
- ³⁰A. Swarup, Ph.D. thesis, University of London, 2007.
- ³¹N. Martucciello and R. Monaco, *Phys. Rev. B* **53**, 3471 (1996).